New Perspective on the Phase Diagram of Cuprate High-Temperature Superconductors

arXiv:1511.02408v1 [cond-mat.supr-con] 7 Nov 2015

Damian Rybicki*
University of Leipzig, Faculty of Physics and Earth Sciences, Linnéstr. 5, 04103 Leipzig, Germany, and
AGH University of Science and Technology, Faculty of Physics and Applied Computer Science, Department of Solid State Physics, al. A. Mickiewicza 30, 30-059 Krakow, Poland
Email: ryba@agh.edu.pl
Tel: +48.12.6172946

Michael Jurkutat
University of Leipzig, Faculty of Physics and Earth Sciences, Linnéstr. 5, 04103 Leipzig, Germany
Email: jurkutat@physik.uni-leipzig.de
Tel: +49.341.9732605

Steven Reichardt
University of Leipzig, Faculty of Physics and Earth Sciences, Linnéstr. 5, 04103 Leipzig, Germany
Email: steven.reichardt@uni-leipzig.de
Tel: +49.341.9732605

Czesław Kapusta
AGH University of Science and Technology, Faculty of Physics and Applied Computer Science, Department of Solid State Physics, al. A. Mickiewicza 30, 30-059 Krakow, Poland
Email: kapusta@agh.edu.pl
Tel: +48.12.6172554

Jürgen Haase
University of Leipzig, Faculty of Physics and Earth Sciences, Linnéstr. 5, 04103 Leipzig, Germany
Email: j.haase@physik.uni-leipzig.de
Tel: +49.341.9732601

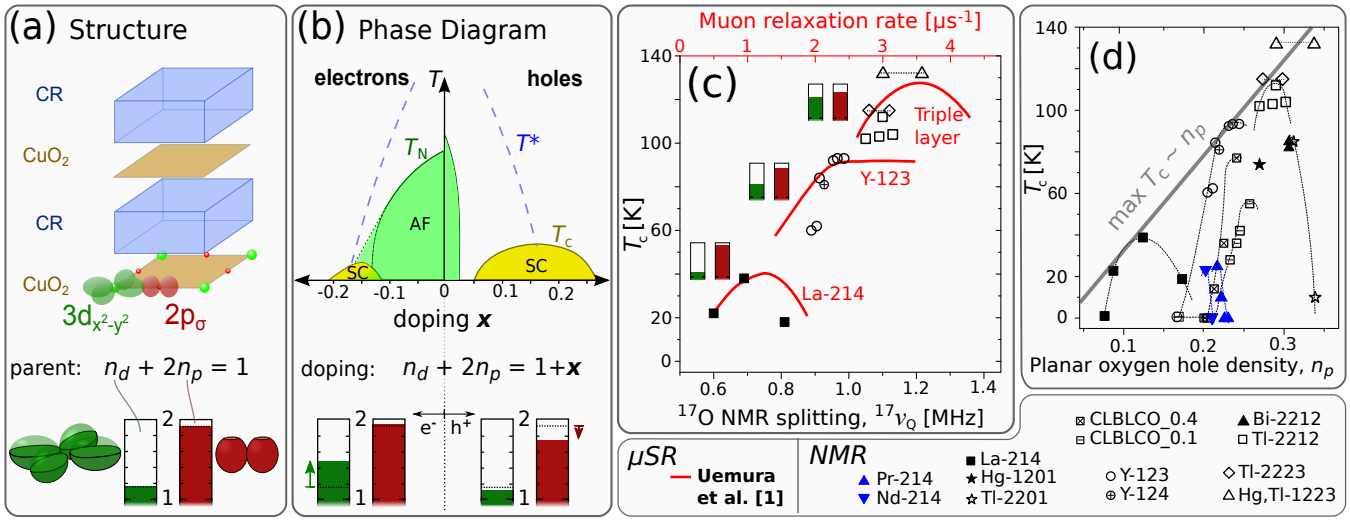

FIG. 1. (a) *top:* the cuprates layered structure has CuO_2 planes and charge reservoir (CR) layers; (a) *bottom:* the bonding orbitals in the CuO_2 plane, i.e., Cu $3d_{x^2-y^2}$ and O $2p_\sigma$, share the nominal Cu $3d$ hole of the Cu^{2+} ion (indicated filling measured with NMR); (b) *top:* schematic electronic phase diagram of the cuprates for electron (*left*) and hole (*right*) doping x, with antiferromagnetic (AF) and superconducting (SC) phases; at low doping the pseudogap reigns below T^*; (b) *bottom:* doped electrons go to the $3d_{x^2-y^2}$ orbital almost exclusively, while doped holes predominantly go to the $2p_\sigma$ orbital; (c) *solid red:* Uemura plot [1], i.e., T_c vs. muon spin relaxation rate (upper abscissa); *black symbols:* T_c vs. planar oxygen quadrupole splitting $^{17}\nu_Q$ (lower abscissa). For triple layer Tl-2223 and Hg,Tl-1223 the pairs connected with a dotted line belong to the same sample and correspond to planar O sites of inner and outer layer (smaller splitting corresponds to underdoped inner CuO_2 layer). (d) T_c vs. planar O hole density n_p calculated from $^{17}\nu_Q$ for all available data (see text).

Universal scaling laws can guide the understanding of new phenomena, and for cuprate high-temperature superconductivity such an early influential relation showed that the critical temperature of superconductivity (T_c) correlates with the density of the superfluid measured at low temperatures. This famous Uemura relation has been inspiring the community ever since. Here we show that the charge content of the bonding orbitals of copper and oxygen in the ubiquitous CuO_2 plane, accessible with nuclear magnetic resonance (NMR), is tied to the Uemura scaling. This charge distribution between copper and oxygen varies between cuprate families and with doping, and it allows us to draw a new phase diagram that has different families sorted with respect to their maximum T_c. Moreover, it also shows that T_c could be raised substantially if we were able to synthesize materials in which more oxygen charge is transferred to the approximately half filled copper orbital.

I. INTRODUCTION

The cuprates' essential building blocks are the CuO_2 plane and charge reservoir layers that separate the planes, cf. Fig. 1(a). While the square-planar CuO_2 plane with a Cu $3d_{x^2-y^2}$ orbital bonding to four O $2p_\sigma$ orbitals is quite universal, the charge reservoir chemistry can vary widely. The antiferromagnetic parent compound can be doped with holes or electrons by alteration of the charge reservoir layers so that the static magnetism vanishes and new electronic phases emerge, cf. Fig. 1(b).

The original plot by Uemura et al. [1] depicted in Fig. 1(c) (in red) shows T_c correlated with the muon spin relaxation rate σ_0 (extrapolated to $T = 0$ K), which is proportional to the superfluid density divided by the effective mass ($\sigma_0 \propto n_s/m^*$). This relation holds for the underdoped materials and nicely orders different cuprate families. This and subsequent scaling laws have remained stimulating up to now, and some were shown to be valid for other superconductors as well [2–10]. Also shown in Fig. 1(c) (in black) is the planar ^{17}O NMR quadrupole splitting ($^{17}\nu_Q$) that measures the O $2p_\sigma$ hole content. The resemblance of this temperature independent charge density at the planar oxygen, set by material chemistry, and σ_0, the density of the superfluid at very low temperatures, is striking.

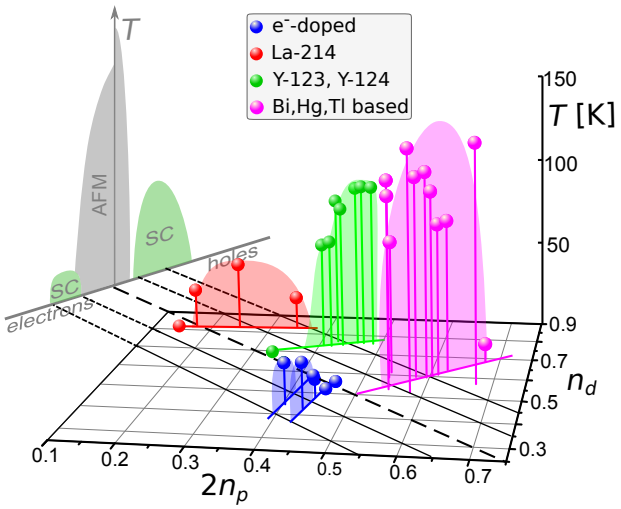

FIG. 2. (Color online) T_c as a function of oxygen ($2n_p$) and copper (n_d) hole content for electron-doped Pr-214 and Nd-214, hole-doped La-214, Y-123 and Bi-, Hg-, Tl-based compounds. The commonly used phase diagram (T vs x) appears as a projection (upper left). Black dashed bold line is for the undoped case (x=0), thin black lines correspond to doping x changing with a step of 0.1.

II. RESULTS AND DISCUSSION

Nuclear magnetic resonance (NMR) as a versatile local bulk probe revealed various trends among certain parameters for the cuprates. [11] However, NMR spin shifts, nuclear relaxation, or local electric field gradients do not lend themselves easily to simple physical pictures. For example, early work related T_c to the planar O and Cu splittings [12], but it did not attract as much interest as the Uemura plot. Subsequent work [13] showed that the splittings are due to the hole content of the Cu $3d_{x^2-y^2}$ (n_d) and O $2p_\sigma$ (n_p) orbitals, and that they measure the chemical hole-doping x (as in $La_{2-x}Sr_xCuO_4$), i.e., $x = \Delta n_d + 2\Delta n_p$. Here, n_d and n_p are measured with NMR based on calibrating the quadrupole splittings with atomic spectroscopy data, in contrast to the earlier model [12]. Very recently [14], it was found that even electron-doping is quantitatively accounted for with n_d and n_p from NMR. In addition, it was found that the parent materials differ substantially in n_d and n_p, however, the relation $n_d + 2n_p = 1$ is obeyed, i.e., the Cu and O bonding orbitals in the CuO_2 plane share the nominal d-shell Cu^{2+} hole differently. This results in the sorting of the families as shown in Fig. 1(d), and one recognizes that a large n_p is a prerequisite for a high maximum T_c (i.e. for optimal doping).

While the knowledge of $^{17}\nu_Q$ is sufficient for calculating n_p, determination of n_d requires the splittings measured at both nuclei [13, 14]. Since NMR can only measure ^{17}O enriched samples, the number of reports on $^{17}\nu_Q$ is much lower compared with $^{63}\nu_Q$ (see Supplementary). Therefore, we could convert all the planar oxygen splittings from the literature, but only the corresponding subset of copper splittings. Although the plot of T_c vs. n_p in Fig. 1(d) is similar to Fig. 1(c), it additionally includes non-superconducting and overdoped compounds. We also recognize in Fig. 1(d) a parabolic-like dependence of T_c on the oxygen charge n_p, which resembles the typical phase diagram that shows a dome-like dependence of T_c on x. Since there is no superfluid in non-superconducting materials (parents, and for doping outside the T_c dome), they cannot be shown in the Uemura plot. Furthermore, the correlation between σ_0 and $^{17}\nu_Q$ is lost in the overdoped regime where σ_0 decreases with increasing doping [15, 16] (which was attributed to a decrease of n_s [17]).

In Fig. 1(d) we also included results for the electron doped materials that we have obtained very recently.[14] For electron-doped $Nd_{1.85}Ce_{0.15}CuO_4$ the muon relaxation rate and the superfluid density were reported to be very similar to that of hole-doped $YBa_2Cu_3O_{6+y}$. [4, 18, 19] We find that μSR data for electron doped compounds are also in agreement with $^{17}\nu_Q$ splittings (see Supplementary) and corresponding hole contents for those families, cf. Fig. 1(d). Electron-doping appears to be less efficient in providing a high T_c, but the rather high oxygen hole content of the parent materials $Pr(Nd)_2CuO_4$ suggests that hole-doping should result in much higher T_c. Clearly, a large n_p is only a prerequisite for a high T_c, but is not sufficient, as expected for such a material chemistry parameter. We also do not know whether this empirical relation remains valid for higher oxygen hole content. If it does, the T_c of the cuprates might be raised by the proper chemistry substantially (we estimate 300 K to 400 K per oxygen hole from the straight line in Fig. 1(d)). Since the charge transfer between Cu and O is governed by $1 = n_d + 2n_p$ for the parent materials, we also conclude that compounds with the highest T_c favor a smaller Cu hole content.

These findings suggest a different kind of cuprate phase diagram that we present in Fig. 2. It does not use the average doping (x) as abscissa, but distinguishes between the oxygen and copper charges. The ordinary phase diagram (T vs. x), cf. Fig. 1(b), appears as a projection that has $x = n_d + 2n_p - 1$ on its abscissa. It must be of great interest to discuss the various cuprate properties probed by other methods in terms of the new phase diagram, however, this task is beyond the scope of this manuscript, and we would like to raise only a few ideas here.

As to the parent compounds, while it is of interest to understand how the exchange coupling J varies as a function of n_d and n_p, the exchange between the CuO_2 planes and with it the Neél temperature will depend on the charge reservoir layers, and correspondingly, T_N shows no simple trend. The parent materials of the electron-doped cuprates promise a large T_c upon *hole* doping.

Doping appears essential for unlocking the maximum T_c, and it changes n_d and n_p in a family-specific manner. While hole-doping changes mostly n_p, electron-doping almost exclusively affects n_d. According to our analysis, all families show optimal doping near $x = n_d + 2n_p - 1 \approx \pm 0.15$. This suggests that optimal doping is related to the parent magnetism rather than the distribution of charges between Cu and O. Electron-doping is less effective in unlocking the maximum T_c. The hole-doped compounds appear in three separate groups: (1) $La_{2-x}Sr_xCuO_4$, (2) $YBa_2Cu_3O_{6+y}$ and other cuprates of that structure, as well as $YBa_2Cu_4O_8$, and (3) Bi, Tl and Hg based families, which have the highest T_c values.

Another important issue concerns the heterogeneity of the cuprates. We know from NMR that the static charge and spin density can vary drastically within the CuO_2 plane, in particular between different cuprate families [20]. For example, the charge density in terms of the total doping x may easily vary by $\Delta x \approx 0.05$[21–23]. Since T_c is not in a simple relation to this static inhomogeneity, only the average n_d and n_p appear to matter. From this, one would conclude that inhomogeneity is either not important for the maximum T_c, or it is ubiquitous and dynamically averaged for NMR, depending on the chemical environment. [20]

Pressure has profound effects on T_c and probably on n_d and n_p. This would be very revealing, and some of us are engaged with new high-pressure NMR experiments [24] and pursue this issue currently.

Concerning the electronic fluid: it is beyond doubt now that the susceptibility of a single electronic spin component cannot explain the cuprate NMR shifts [25, 26]. Instead, one needs at least a Fermi-liquid-like spin component that has a temperature-independent spin polarization above T_c, and a pseudogap-like spin component that is temperature-dependent far above T_c for lower doping levels. A third, doping-dependent NMR shift term was recently identified [27], and it may represent the expected coupling between the two components. Therefore, it will be of great interest to see how the different spin components vary across the new phase diagram.

To conclude, NMR measures the charge distribution in the bonding orbitals in the CuO_2 plane quantitatively, and since it reproduces the Uemura plot, i.e., it finds the same ordering of families with respect to their maximum T_c, we now have material chemistry parameters that are responsible for setting the highest T_c and superfluid density. These findings inspired a new perspective on the cuprate phase diagram and it is very likely that the complex cuprate properties might be better understood when discussed in the context of the charge distribution in the CuO_2 plane.

ACKNOWLEDGMENTS

Acknowledgement We are thankful to O.P. Sushkov, C. P. Slichter, G. V. M. Williams for helpful discussions, and acknowledge financial support by the University of Leipzig, the DFG within the Graduate School Build-MoNa, the European Social Fund (ESF) and the Free State of Saxony.

[1] Y. J. Uemura, G. M. Luke, B. J. Sternlieb, J. H. Brewer, J. F. Carolan, W. N. Hardy, R. Kadono, J. R. Kempton, R. F. Kiefl, S. R. Kreitzman, P. Mulhern, T. M. Riseman, D. L. Williams, B. X. Yang, S. Uchida, H. Takagi, J. Gopalakrishnan, A. W. Sleight, M. A. Subramanian, C. L. Chien, M. Z. Cieplak, G. Xiao, V. Y. Lee, B. W. Statt, C. E. Stronach, W. J. Kossler, and X. H. Yu, Phys. Rev. Lett. **62**, 2317 (1989).

[2] S. V. Dordevic, E. J. Singley, D. N. Basov, S. Komiya, Y. Ando, E. Bucher, C. C. Homes, and M. Strongin, Phys. Rev. B **65**, 134511 (2002).

[3] A. T. Savici, Y. Fudamoto, I. M. Gat, T. Ito, M. I. Larkin, Y. J. Uemura, G. M. Luke, K. M. Kojima, Y. S. Lee, M. A. Kastner, R. J. Birgeneau, and K. Yamada, Phys. Rev. B **66**, 014524 (2002).

[4] C. C. Homes, S. V. Dordevic, M. Strongin, D. A. Bonn, R. Liang, W. N. Hardy, S. Komiya, Y. Ando, G. Yu, N. Kaneko, X. Zhao, M. Greven, D. N. Basov, and T. Timusk, Nature **430**, 539 (2004).

[5] J. L. Tallon, J. R. Cooper, S. H. Naqib, and J. W. Loram, Phys. Rev. B **73**, 180504 (2006).

[6] C. C. Homes, Phys. Rev. B **80**, 180509 (2009).

[7] S. V. Dordevic, D. N. Basov, and C. C. Homes, Sci. Rep. **3**, 1713 (2013).

[8] D. Wu, N. Barii, N. Drichko, P. Kallina, A. Faridian, B. Gorshunov, M. Dressel, L. Li, X. Lin, G. Cao, and Z. Xu, Physica C **470**, S399 (2010).
[9] C. C. Homes, Z. J. Xu, J. S. Wen, and G. D. Gu, Phys. Rev. B **86**, 144530 (2012).
[10] A. Shengelaya and K. A. Mller, EPL **109**, 27001 (2015).
[11] C. P. Slichter, Handbook of High-Temperature Superconductivity, edited by J. R. Schrieffer (Springer, 2007).
[12] G. Zheng, Y. Kitaoka, K. Ishida, and K. Asayama, J. Phys. Soc. Jpn. **64**, 2524 (1995).
[13] J. Haase, O. P. Sushkov, P. Horsch, and G. Williams, Phys. Rev. B **69**, 0945041 (2004).
[14] M. Jurkutat, D. Rybicki, O. P. Sushkov, G. V. M. Williams, A. Erb, and J. Haase, Phys. Rev. B **90**, 140504 (2014).
[15] Y. J. Uemura, A. Keren, L. P. Le, G. M. Luke, W. D. Wu, Y. Kubo, T. Manako, Y. Shimakawa, M. Subramanian, J. Cobb, and J. Markert, Nature **364**, 605 (1993).
[16] C. Niedermayer, C. Bernhard, U. Binninger, H. Glückler, J. L. Tallon, E. J. Ansaldo, and J. I. Budnick, Phys. Rev. Lett. **71**, 1764 (1993).
[17] J. L. Tallon, C. Bernhard, and C. Niedermayer, Supercond. Sci. Technol. **10**, A38 (1997).
[18] A. Shengelaya, R. Khasanov, D. G. Eshchenko, D. Di Castro, I. M. Savić, M. S. Park, K. H. Kim, S.-I. Lee, K. A. Müller, and H. Keller, Phys. Rev. Lett. **94**, 127001 (2005).
[19] C. C. Homes, B. P. Clayman, J. L. Peng, and R. L. Greene, Phys. Rev. B **56**, 5525 (1997).
[20] J. Haase, Phys. Rev. Lett. **91**, 189701 (2003).
[21] D. Rybicki, J. Haase, M. Greven, G. Yu, Y. Li, Y. Cho, and X. Zhao, J. Supercond. Nov. Magn. **22**, 179 (2009).
[22] M. Jurkutat, J. Haase, and A. Erb, J. Supercond. Nov. Magn. **26**, 2685 (2013).
[23] P. M. Singer, A. W. Hunt, and T. Imai, Phys. Rev. Lett. **88**, 047602 (2002).
[24] T. Meissner, S. K. Goh, J. Haase, G. V. M. Williams, and P. B. Littlewood, Phys. Rev. B **83**, 220517 (2011).
[25] J. Haase, C. P. Slichter, and G. V. M. Williams, J. Phys.: Condens. Matter **21**, 455702 (2009).
[26] J. Haase, D. Rybicki, C. P. Slichter, M. Greven, G. Yu, Y. Li, and X. Zhao, Phys. Rev. B **85**, 104517 (2012).
[27] D. Rybicki, J. Kohlrautz, J. Haase, M. Greven, X. Zhao, M. K. Chan, C. J. Dorow, and M. J. Veit, arXiv:1505.01725v1.

Supplement to: New Perspective on the Phase Diagram of Cuprate High-Temperature Superconductors

arXiv:1511.02408v1 [cond-mat.supr-con] 7 Nov 2015

Damian Rybicki*
University of Leipzig, Faculty of Physics and Earth Sciences, Linnestr. 5, 04103 Leipzig, Germany, and
AGH University of Science and Technology, Faculty of Physics and Applied Computer Science, Department of Solid State Physics, al. A. Mickiewicza 30, 30-059 Krakow, Poland
Email: ryba@agh.edu.pl
Tel: +48.12.6172946

Michael Jurkutat
University of Leipzig, Faculty of Physics and Earth Sciences, Linnestr. 5, 04103 Leipzig, Germany
Email: jurkutat@physik.uni-leipzig.de
Tel: +49.341.9732605

Steven Reichardt
University of Leipzig, Faculty of Physics and Earth Sciences, Linnestr. 5, 04103 Leipzig, Germany
Email: steven.reichardt@uni-leipzig.de
Tel: +49.341.9732605

Czesław Kapusta
AGH University of Science and Technology, Faculty of Physics and Applied Computer Science, Department of Solid State Physics, al. A. Mickiewicza 30, 30-059 Krakow, Poland
Email: kapusta@agh.edu.pl
Tel: +48.12.6172554

Jürgen Haase
University of Leipzig, Faculty of Physics and Earth Sciences, Linnestr. 5, 04103 Leipzig, Germany
Email: j.haase@physik.uni-leipzig.de
Tel: +49.341.9732601

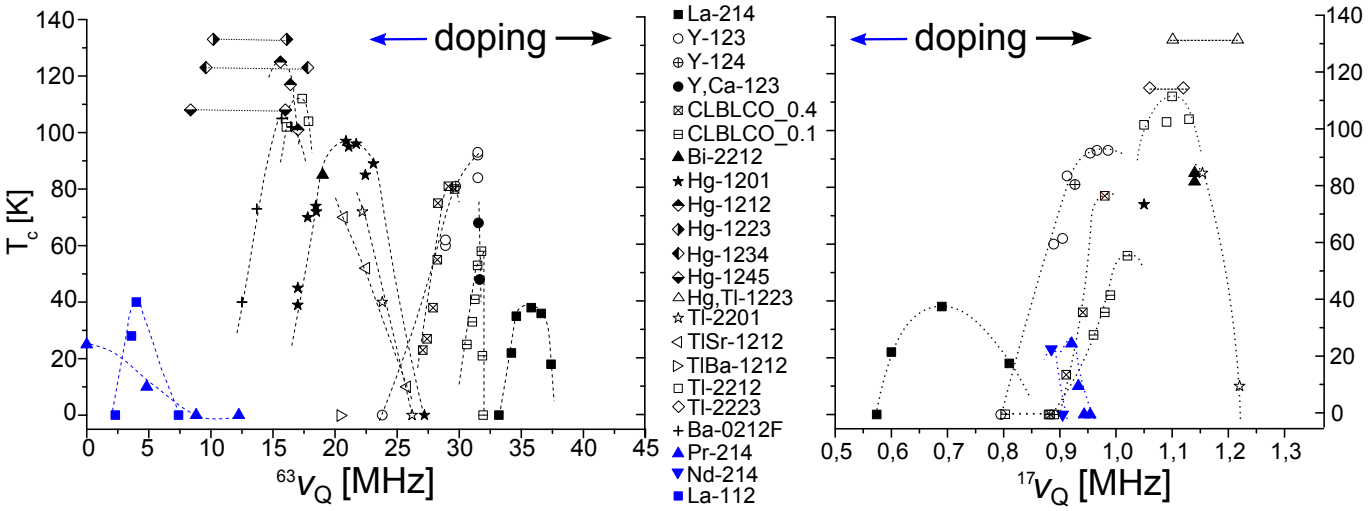

FIG. 1. (Color online) Phase diagrams of cuprates based on quadrupole splittings of the planar copper (*left panel*) and oxygen (*right panel*). Black and blue symbols and arrows (indicating increase of doping x) are for hole and electron doped systems, respectively. Dotted lines are guides to the eye and connect different doping levels for one family. For compounds with three or more CuO_2 layers there are two different planar Cu and O sites, which have different quadrupole splittings, hence the horizontally connected data points belong to the same sample.

A detailed analysis of the planar oxygen and copper electric field gradient tensors in the cuprates is presented elsewhere [1]. Here we only present collected literature values of the quadrupole splittings of planar copper $\left(^{63}\nu_Q\right)$ and oxygen $(^{17}\nu_Q)$ (table 1 and 2, respectively). All ^{17}O and most of ^{63}Cu splittings are also plotted in Fig. 1. In the case of the CLBLCO family there are $^{63}\nu_Q$ data for more dopings.[2] Since all show the same behaviour in the tables we show only two families, for which both $^{63}\nu_Q$ and $^{17}\nu_Q$ are available. There are also $^{63}\nu_Q$ results for cuprates containing Bi, e.g. for single layer Bi-2201 family.[3] However, the ^{63}Cu NQR spectra are very broad with at least four peaks (ranging from 27 MHz to 35 MHz), despite the fact that all Cu sites are equivalent in the ideal Bi-2201 structure without the modulation in the Bi-O layer. Very broad ^{63}Cu NQR spectra are a general feature of cuprates with this type of modulation [4], and we only quote one $^{63}\nu_Q$ obtained from NMR on Bi-2212 single crystals,[5] for which also $^{17}\nu_Q$ is available.

The hole contents of the oxygen $2p_\sigma$ (n_p) and copper $3d_{x^2-y^2}$ (n_d) orbitals, which are shown in the main paper, are calculated using the following formulas [6]:

$$n_p = \frac{^{17}\nu_Q - 0.39 \text{ MHz}}{2.45 \text{ MHz}}$$

$$n_d = \frac{^{63}\nu_Q + 5.65(8 - 4n_p) \text{ MHz}}{94.3 \text{ MHz}}.$$

[1] D. Rybicki, M. Jurkutat, S. Reichardt, and J. Haase, arXiv:1402.4014v1.
[2] A. Keren, A. Kanigel, and G. Bazalitsky, Phys. Rev. B **74**, 172506 (2006).
[3] Y. Masaki, K.and Kazuyoshi and K. Koji, J. Solid State Chem. **133**, 372 (1997).
[4] I. Lipinski, A. Zalessky, A. Levanyuk, G. Mironova, E. Smirnovskaya, and A. Bush, Physica C **168**, 291 (1990).
[5] K. Ishida, Y. Kitaoka, K. Asayama, K. Kadowaki, and T. Mochiku, J. Phys. Soc. Jpn. **63**, 1104 (1994).
[6] M. Jurkutat, D. Rybicki, O. P. Sushkov, G. V. M. Williams, A. Erb, and J. Haase, Phys. Rev. B **90**, 140504 (2014).
[7] J. Haase, O. P. Sushkov, P. Horsch, and G. V. M. Williams, Phys. Rev. B **69**, 094504 (2004).
[8] K. Fujiwara, Y. Kitaoka, K. Ishida, K. Asayama, Y. Shimakawa, T. Manako, and Y. Kubo, Physica C **184**, 207 (1991).
[9] K. Magishi, Y. Kitaoka, G.-q. Zheng, K. Asayama, T. Kondo, Y. Shimakawa, T. Manako, and Y. Kubo, Phys. Rev. B **54**, 10131 (1996).
[10] T. Goto, S. Nakajima, M. Kikuchi, Y. Syono, and T. Fukase, Phys. Rev. B **54**, 3562 (1996).
[11] A. Gerashenko, Y. Piskunov, K. Mikhalev, A. Ananyev, K. Okulova, S. Verkhovskii, A. Yakubovskii, L. Shustov, and A. Trokiner, Physica C **328**, 163 (1999).
[12] Z. Han, R. Dupree, R. Liu, and P. Edwards, Physica C **226**, 106 (1994).
[13] G. V. M. Williams, S. Kramer, and M. Mehring, Phys. Rev. B **63**, 104514 (2001).
[14] G. Zheng, Y. Kitaoka, K. Asayama, K. Hamada, H. Yamauchi, and S. Tanaka, Physica C **260**, 197 (1996).
[15] A. A. Gippius, E. V. Antipov, W. Hoffmann, and K. Luders, Physica C **276**, 57 (1997).
[16] S. Shimizu, S. Iwai, S. Tabata, H. Mukuda, Y. Kitaoka, P. M. Shirage, H. Kito, and A. Iyo, Phys. Rev. B **83**, 144523 (2011).
[17] D. R. et. al, unpublished.
[18] D. Rybicki, J. Haase, M. Lux, M. Jurkutat, M. Greven, G. Yu, Y. Li, and X. Zhao, arXiv:1208.4690 (2012).
[19] D. Rybicki, J. Haase, M. Greven, G. Yu, Y. Li, Y. Cho, and X. Zhao, J. Supercond. Nov. Magn. **22**, 179 (2009).
[20] S. Ohsugi, T. Tsuchiya, T. Koyama, and K. Fueki, J. Low Temp. Phys. **105**, 419 (1996).
[21] M. Horvatic, C. Berthier, P. Carretta, J. Gillet, P. Sgransan, Y. Berthier, and J. Capponi, Physica C **235**, 1669 (1994).
[22] M.-H. Julien, M. Horvatic, P. Carretta, C. Berthier, Y. Berthier, P. Segransan, S. Loureiro, and J.-J. Capponi, Physica C **268**, 197 (1996).
[23] M.-H. Julien, M. Horvatic, C. Berthier, and P. Segransan, J. Low Temp. Phys. **105**, 371 (1996).
[24] K. Magishi, Y. Kitaoka, G.-q. Zheng, K. Asayama, K. Tokiwa, A. Iyo, and H. Ihara, Phys. Rev. B **53**, R8906 (1996).
[25] H. Breitzke, I. Eremin, D. Manske, E. Antipov, and K. Luders, Physica C **406**, 27 (2004).
[26] K. Mikhalev, K. Kumagai, Y. Furukawa, V. Bobrovskii, T. Dyachkova, N. Kadirova, and A. Gerashenko, Physica C **304**, 165 (1998).
[27] K. Itohara, S. Shimizu, H. Mukuda, Y. Kitaoka, P. M. Shirage, H. Kito, and A. Iyo, Physica C **470**, S140 (2010).
[28] T. Imai, C. Slichter, J. Cobb, and J. Markert, J. Phys. Chem. Solids **56**, 1921 (1995).
[29] H. Kotegawa, Y. Tokunaga, Y. Araki, G.-q. Zheng, Y. Kitaoka, K. Tokiwa, K. Ito, T. Watanabe, A. Iyo, Y. Tanaka, and H. Ihara, Phys. Rev. B **69**, 014501 (2004).
[30] A. M. Mounce, S. Oh, J. A. Lee, W. P. Halperin, A. P. Reyes, P. L. Kuhns, M. K. Chan, C. Dorow, L. Ji, D. Xia, X. Zhao, and M. Greven, Phys. Rev. Lett. **111**, 187003 (2013).
[31] S. Kambe, H. Yasuoka, A. Hayashi, and Y. Ueda, Phys. Rev. B **47**, 2825 (1993).
[32] G. Zheng, Y. Kitaoka, K. Ishida, and K. Asayama, J. Phys. Soc. Jpn. **64**, 2524 (1995).
[33] M. Takigawa and D. B. Mitzi, Phys. Rev. Lett. **73**, 1287 (1994).
[34] J. Crocker, A. P. Dioguardi, N. Roberts-Warren, A. C. Shockley, H.-J. Grafe, Z. Xu, J. Wen, G. Gu, and N. J. Curro, Phys. Rev. B **84**, 224502 (2011).
[35] A. Trokiner, K. Mikhalev, A. Yakubovskii, P.-V. Bellot, S. Verkhovskii, Y. Zhdanov, Y. Piskunov, L. Shustov, A. Inyushkin, and A. Taldenkov, Physica C **255**, 204 (1995).
[36] K. Lim, H. Lee, and N. Hur, Physica C **232**, 215 (1994).
[37] E. Amit and A. Keren, Phys. Rev. B **82**, 172509 (2010).

TABLE I. ^{63}Cu quadrupole splitting $^{63}\nu_Q$ for various families of cuprates in order of increasing doping ("und." - underdoped, "opt." - close to optimal doping, "ovd." - overdoped). For Tl- and Hg- families with three or more CuO_2 layers there are two Cu sites, the inner layer with Cu(1) and the outer layer Cu(2).

Family	T_c [K]	$^{63}\nu_Q$ [MHz]	Family	T_c [K]	$^{63}\nu_Q$ [MHz]
La-214 ref.[7]	0	33.2	Bi-2212	86 (opt) ref.[5]	19.0
	22	34.2	Tl-2201 ref.[8]	72 (ovd)	22.2
	35	34.6		40 (ovd)	23.8
	38	35.8		0 (ovd	26.2
	36	36.6	TlSr-1212 ref.[9]	70 (ovd)	20.7
	18	37.4		52 (ovd)	22.5
Y-123 ref.[7]	0	23.8		10 (ovd)	25.8
	60	28.9	TlBa-1212 ref.[10]	0	20.44
	62	28.9	Tl-2212 ref.[11]	102 (und)	16.08
	84	31.5		112 (opt)	17.35
	92	31.5		104 (ovd)	17.87
	93	31.5	Tl-2223 Cu(1)	125 (opt) ref.[12]	11.7
Y-124 ref.[7]	81	29.72	Cu(2)		16.4
Y,Ca-123 ref.[13]	68 (ovd)	31.55	Cu(1)	115 (ovd?) ref.[14]	10.8
	48 (ovd)	31.65	Cu(2)		17.4
Hg-1201	39 (und) ref.[15]	17.0	Ba-0212F ref.[16]	40 (und)	12.5
	45 (und) ref.[17]	17.0		73 (und)	13.7
	70 (und) ref.[15]	17.8		105 (opt)	15.7
	72 (und) ref.[15]	18.5		102 (ovd)	16.5
	74 (und) ref.[18]	18.46	CLBLCO_0.1 ref.[2]	25 (und)	30.6
	95 (opt) ref.[15]	21.1		41 (und)	31.2
	96 (opt) ref.[15]	21.7		58 (opt)	31.8
	97 (opt) ref.[19]	20.88		21 (ovd)	31.87
	89 (ovd) ref.[15]	23.1		0 (ovd)	31.93
	85 (ovd) ref.[17]	22.4	CLBLCO_0.4 ref.[2]	23 (und)	27.1
	0 (ovd) ref.[15]	27.2		38 (und)	27.9
Hg-1212	125 (opt) ref.[20]	15.6		75 (und)	28.3
	117 (ovd) ref.[20]	16.4		81 (opt)	29.1
	101 (ovd) ref.[21]	17.0	Pr-214 ref.[6]	0	12.2
	101 (ovd) ref.[22]	17.6		0	8.8
Hg-1223 Cu(1)	115 (und) ref.[23]	9.7		10 (und)	4.8
Cu(2)		13.7		25 (opt)	0
Cu(1)	133 (opt) ref.[24]	10.2	Nd-214 ref.[6]	0	14
Cu(2)		16.1		25 (opt)	1
Hg,Cu-1223 Cu(1)	134 (opt) ref.[25]	15.3	La -112	0 ref.[26]	7.4
Cu(2)		16.6		28 (und) ref.[26]	3.6
Hg-1234 Cu(1)	85 (und) ref.[27]	9.3		40 (opt) ref.[28]	≤4
Cu(2)		14.8		0 (ovd) ref.[26]	2.3
Cu(1)	123 (opt) ref.[27]	9.6			
Cu(2)		17.8			
Hg-1245 Cu(1)	108 (opt) Ref.[29]	8.37			
Cu(2)		16			

TABLE II. Quadrupole splitting $^{17}\nu_Q$ of planar oxygen for various families of cuprates in order of increasing doping ("und." - underdoped, "opt." - close to optimal doping, "ovd." - overdoped). For Tl- and Hg- families with three or more CuO_2 layers there are two planar O sites, the inner layer with O(1) and the outer layer O(2).

Family	T_c [K]	$^{17}\nu_Q$ [MHz]
La-214 ref.[7]	0	0.574
	22	0.6
	38 (opt)	0.69
	18	0.81
Y-123 ref.[7]	0	0.795
	60	0.889
	62	0.905
	84	0.913
	92	0.954
	93 (opt)	0.986
	93 (opt)	0.966
Y-124 ref.[7]	81	0.927
Hg-1201 ref.[30]	74 (und)	1.050
Tl-2201 ref.[31, 32]	85 (opt)	1.154
	10 (ovd)	1.220
Bi-2212 ref.[33, 34]	86 (opt)	1.14
	82 (ovd)	1.14
TlSr-2212	102 (und) ref.[11]	1.05
	112 (opt) ref.[11]	1.10
	104 (ovd) ref.[11]	1.13
	103 (ovd) ref.[35]	1.09
Tl-2223 O(1)	115 (ovd?) ref.[14]	1.06
O(2)		1.12
Hg,Tl-1223 O(1)	132 (opt) ref.[36]	1.101
O(2)		1.217
CLBLCO_0.1 ref.[37]	0	0.8
	0	0.89
	28	0.96
	36	0.98
	42	0.99
	55 (opt)	1.02
CLBLCO_0.4 ref.[37]	0	0.88
	14	0.91
	36	0.94
	77 (opt)	0.98
Pr-214 ref.[6]	0	0.905
	0	0.943
	10	0.933
	25 (opt)	0.921
Nd-214 ref.[6]	0	0.905
	23 (opt)	0.885